HHS Public Access

Author manuscript

Magn Reson Imaging. Author manuscript; available in PMC 2016 September 01.

Published in final edited form as:

Magn Reson Imaging. 2015 September ; 33(7): 895–902. doi:10.1016/j.mri.2015.05.003.

Detection of Hand and Leg Motor Tract Injury Using Novel Diffusion Tensor MRI Tractography in Children with Central Motor Dysfunction

Jeong-Won Jeong[a,b,c,*], **Jessica Lee**[d], **David O. Kamson**[a], **Harry T. Chugani**[a,b,c], and **Csaba JuhÁsz**[a,b,c]

[a]Translational Imaging Laboratory, Children's Hospital of Michigan, Detroit, MI, USA

[b]Carman and Ann Adams Department of Pediatrics, School of Medicine, Wayne State University, Detroit, MI, USA

[c]Department of Neurology, School of Medicine, Wayne State University, Detroit, MI, USA

[d]School of Medicine, Wayne State University, Detroit, MI, USA

Abstract

Purpose—To examine whether an objective segmenation of corticospinal tract (CST) associated with hand and leg movements can be used to detect central motor weakness in the corresponding extremities in a pediatric population.

Material and Methods—This retrospective study included diffusion tensor imaging (DTI) of 25 children with central paresis affecting at least one limb (age: 9.0±4.2 years, 15 boys, 5/13/7 children with left/right/both hemispheric lesions including ischemia, cyst, and gliosis), as well as 42 pediatric control subjects with no motor dysfunction (age: 9.0±5.5 years, 21 boys, 31 healthy/11 non-lesional epilepsy children). Leg- and hand-related CST pathways were segmented using DTI-maximum *a posteriori* (DTI-MAP) classification. The resulting CST volumes were then divided by total supratentorial white matter volume, resulting in a marker called “normalized streamline volume ratio (NSVR)” to quantify the degree of axonal loss in separate CST pathways associated with leg and hand motor functions. A receiver operating characteristic curve was applied to measure the accuracy of this marker to identify extremities with motor weakness.

Results—NSVR values of hand/leg CST selectively achieved the following values of accuracy/sensitivity/specificity: 0.84/0.84/0.57, 0.82/0.81/0.55, 0.78/0.75/0.55, 0.79/0.81/0.54 at a cut-off of 0.03/0.03/0.03/0.02 for right hand CST, left hand CST, right leg CST, and left leg CST, respectively. Motor weakness of hand and leg was most likely present at the cut-off values of hand

[*]Corresponding author: Jeong-Won Jeong, Ph.D., Departments of Pediatrics and Neurology, Wayne State University, School of Medicine, PET Center and Translational Imaging Laboratory, Children's Hospital of Michigan, 3901 Beaubien St., Detroit, MI, 48201, Phone: 313-993-0258 Fax: 313-966-9228, jeongwon@pet.wayne.edu.

The authors declare no conflicts of interest.

and leg NSVR (i.e., 0.029/0.028/0.025/0.020 for left-hand/right-hand/left-leg/right-leg). The control group showed a moderate age-related increase in absolute CST volumes and a biphasic age-related variation of the normalized CST volumes, which were lacking in the paretic children.

Conclusions—This study demonstrates that DTI-MAP classification may provide a new imaging tool to quantify axonal loss in children with central motor dysfunction. Using this technique, we found that early-life brain lesions affect the maturational trajectory of the primary motor pathway which may be used as an effective marker to facilitate evidence-based treatment of paretic children.

Keywords

Diffusion tensor imaging; corticospinal tract; volume; children; hemiparesis; brain maturation

1. Introduction

Hemiparesis is defined as weakness of one vertical side of the body due to injury to the central nervous system. In most cases, the injury occurs to the side of the brain contralateral to the affected limbs. Its most severe form is known as hemiplegia, which entails full paralysis of the muscles in the affected side [1,2]. Bilateral paresis can develop if the primary motor cortex or motor pathways are injured bilaterally (tetraparesis). There is a wide range of injuries that can cause central paresis in children, such as peri- or postnatal stroke, brain trauma, or genetic/metabolic disorders [3]. In general, such injuries occur in 1 out of every 500 births, whereas the incidence highly increases with low birth weight and prematurity, but can also be acquired later in life [4]. Such injuries present significant challenges in the rehabilitation and education of the affected children; thus, there is a great demand for an imaging marker that could objectively assess severity of structural motor abnormalities, predict future development of motor function and monitor effects of therapy for these patients.

Diffusion tensor imaging (DTI) tractography is a well established imaging technique that quantifies water diffusivity along the axons, enabling *in vivo* study of neural pathways including the corticospinal tract (CST) [6-10]. CST connects the motor cortex to the spinal cord enabling voluntary motor control over the limbs [11]. In previous DTI studies, CST was evaluated as a whole. This approach, while informative, does not account for possible discrepancies in the degree of injury to leg and hand related fibers, thus significantly masking the measures of DTI in the regions of interest. To overcome this critical problem, we recently developed a new method, independent component analysis combined with ball-stick model (ICA+BSM) allowing identification and isolation of crossing fibers related to control of the hands and legs [12-15]. Using this approach, it was found that in children with unilateral brain damage due to Sturge-Weber syndrome, hand-related (but not leg-related) CST volumes were consistently decreased in the affected hemisphere [16]. Follow-up showed that depending on the level of brain damage, varying degrees of compensation occurred as reflected by changes in CST volume [16]. Another study demonstrated that asymmetries also exist between the development of hand- and leg- related fibers of the CST in typically developing children [17]. In the present study, we postulated that DTI tractography may provide additional information about the development of CST in children

with central motor weakness, and that the presence of DTI abnormalities would reflect the pattern of motor weakness in the affected hands and legs.

This study aims to investigate a new tool using DTI tractography, which can objectively evaluate axonal loss (and plasticity) of primary motor functions in children with paresis. A novel method called “diffusion tensor imaging maximum *a posteriori* probability” (DTI-MAP) classifier was utilized to identify two prominent subdivisions of the CST [14,15], which are associated with hand/arm and leg/trunk motor control. The volumes of resulting CST segments were analyzed with respect to the presence and distribution of motor weakness determined by clinical neurological examination. We postulated that paretic children would show significantly decreased CST fiber volumes in the affected hemisphere, when compared to corresponding CST volumes of age-matched non-paretic controls,. Also, it was postulated that the decreased fiber volumes of the hand- and leg-related CST segments would correlate with the deficit in the corresponding limbs.

2. Materials and Methods

2.1. Subjects

The present study is a retrospective observational on 25 children with motor weakness of central origin, either unilateral or bilateral in either the hands and/or legs (23 children also had increased muscle tone documented in the affected extremity; age: 1.5-16.5 years, mean age: 9.0±4.2 years, 15 boys, 8/7/9/1 right/left/bi-handedness/unknown) and 42 control subjects (age: 1.8-19.0 years, mean age: 9.0±5.5 years, 21 boys, 28/7/2/5 right/left/bi-handedness/unknown) including 31 children with typical development (mean age 11.2±4.7 years) and 11 children with new onset epilepsy but having no structural abnormalities on MRI and no motor impairment (mean age: 2.7±0.6 years). Age and gender did not differ between central motor deficit (MD) and control groups (p=0.39 and 0.28, respectively).

The patients with MD were recruited through the pediatric neurology clinics at Children's Hospital of Michigan with the following criteria: 1) having motor weakness in at least one extremity. 2) having no known genetic disorders and 3) having no severe comorbidities (e.g., severe intellectual disability). Based on the above criteria, we included 5/13/7 children with left/right/both hemispheric lesions including ischemia, cyst, and gliosis confirmed by MRI. Among them 14 children had epilepsy and 13 were developmentally delayed. MD children were categorized into 4 subgroups according to their distribution of motor weakness associated with each body part as listed in Table 1. Time interval between the initial diagnosis and MRI was 1.3±1.7 years. None of the control subjects had motor weakness on neurological examination. The Human Investigations Committee (HIC) of Wayne State University granted permission for performing MRIs (without sedation) in children with typical development, and parents signed an informed consent form. We had also permission from the HIC to use clinically acquired MRI scans after deidentification. The 25 patients with MD and 11 patients with focal epilepsy were sedated for clinical MRI acquisition.

2.2. MRI acquisition

MR scans were performed using a 3T GE-Signa scanner (GE Healthcare, Milwaukee, WI) equipped with an 8-channel head coil and ASSET. DTI was acquired with a multi-slice single shot diffusion weighted echo-planar-imaging (EPI) sequence at repetition time = 12,500 ms, echo time = 88.7 ms, field of view (FOV) = 240 mm, 128×128 acquisition matrix (nominal resolution = 1.89 mm), contiguous 3 mm thickness in order to cover entire axial slices of the whole brain using 55 isotropic gradient directions with b= 1000s/mm^2, one b=0 acquisition, and number of excitations = 1. Children with neurological conditions being scanned clinically were sedated, if needed, using pentobarbital (3 mg/kg) followed by fentanyl (1μg/kg).

2.3. DTI-MAP classification

Whole brain tractography was performed using ICA+BSM to reconstruct streamlines of white matter fibers, as described and validated recently in various pediatric patient groups using functional MRI and invasive electrical stimulation mapping symptoms [12,13]. In brief, the orientations of up to three stick compartments[26] were identified at each voxel using the ICA+BSM The resulting orientations were interpolated to track ongoing fibers using deterministic streamline tractography parameterized at fractional ratio ≥ 0.1, deflection angle ≤ 60°, and step size=0.5 voxel width. To identify the two segments of CST streamlines associated with primary motor pathways of the hand and leg, DTI-MAP classifier was applied, which can automatically classify individual streamlines into one of three segments, hand, leg, and face, based on their stereotactic atlases constructed from healthy children [14,15]. For each segment, a streamline visitation map was created by using the number of streamlines passing through each voxel. Voxels having at least 1 visit were assumed to belong to each motor pathway. Streamline volume was measured by the total volume of all voxels belonging to the segment. Finally, *normalized* streamline volume ratios (NSVR) of the hand and leg segments were obtained in each hemisphere by dividing the corresponding streamline volume to total white matter volume of both cerebral hemispheres (i.e., excluding cerebellum).

2.4. Statistical Analysis

To investigate the group differences between controls and MD subgroups listed in Table 1, separate univariate analyses of variance (ANOVA) were applied for four NSVR values (i.e., hand and leg CST segments in both hemispheres). For these analyses, both age and gender were included as covariates. Receiver operating characteristic (ROC) analyses were used to test four NSVR values as diagnostic measures identifying (or predicting) the presence or absence of motor weakness in corresponding body parts. Cut-off values of four NSVR measures were found to maximize the accuracy of diagnostic evaluative outcomes obtained from DTI-MAP classifications. Finally, both absolute CST volume and NSVR values of each CST segment were plotted against the patients' age. Based on the apparent nonlinear relationship, NSVR values were also fitted to analytic functions of cascade exponential curves in order to investigate age-related CST changes. All statistical analyses were carried out using the SPSS Statistics 21.0 software (SPSS Inc, Somers, New York). P-values < .05 were considered statistically significant.

3. Results

Figure 1 shows representative examples of DTI-MAP classifications to detect separate CST segments connecting the primary motor cortex of hand and leg to the internal capsule in age-matched healthy controls and MD children. Compared with healthy controls, MD children showed striking decreases of the streamline volumes of hand and leg CST fibers in the affected hemisphere corresponding to motor weakness of hand and leg in the opposite side (Table 1).

Univariate ANOVA demonstrated significantly decreased normalized volumes of hand and leg CST segments in all MD subgroups compared with the healthy controls (Figure 2 and Table 2), Compared with healthy controls, the most significant decrease was found in MD_1 having the most extensive motor weakness (in both hand and leg on both sides). In the other subgroups, decreased NSVR values of the affected CST segments were more apparent contralateral to the motor weakness of the corresponding extremity on the opposite side. Specifically, in the MD_2 group, with motor weakness in the left hand and leg, a more significant decrease (lower p values) in NSVR values of hand and leg CST segments of the right hemisphere was seen. In MD_3, with motor weakness in the right hand and leg, patients showed significant decrease in NSVR value in the corresponding leg CST segments and a strong trend in NSVR value of hand CST segment of the left hemisphere. In MD_4, with motor weakness in both hands (but not legs), both hand CST segments (but not the leg segments) showed a trend for decreased NSVR values.

The subsequent ROC analyses demonstrated that the NSVR values of the hand and leg CST segments could be used as reliable imaging markers to detect the existence of motor weakness on the opposite side (Figure 3). Area under curve (AUC) values to predict motor weakness were 0.8615/0.8432/0.7823/0.8181 for right hand CST, left hand CST, right leg CST, and left leg CST, respectively. The accuracy/sensitivity/specificity values to predict motor weakness were 0.84/0.84/0.57, 0.82/0.81/0.55, 0.78/0.75/0.55, 0.79/0.81/0.54 at a cut-off of 0.0296/0.0279/0.0247/0.0202 for right hand CST, left hand CST, right leg CST, and left leg CST, respectively.

Plots of absolute values of total white matter volume and CST segmental volumes by age showed a moderate age-related increase in the control group (R^2 values below 0.3 in all CST correlations), but a mild decline in the paretic group, thus creating an increasing gap between the two groups as age increased (Figure 4); this decline reached significance only in the right leg CST ($p=0.02$). Plots of normalized CST volumes by age showed that, in controls, each of the four NSVR values showed an early age-related increase, then a plateau around age 5 years, followed by a exponential decline until age 10-12 (depending on the actual CST segment; $R^2 = 0.269$, $p=0.0003$ for left hand CST; $R^2 = 0.308$, $p=0.001$ for right hand CST; $R^2 = 0.199$, $p=0.0025$ for left leg CST; $R^2 = 0.559$, $p<0.0001$ for right leg CST) (Figure 5). In contrast, none of the four NSVR values showed any significant trend with age in MD children, suggesting no prominent age-related change in the CST volumes.

4. Discussion

The results of this study demonstrate that DTI-MAP classification of hand/leg CST may provide a novel neuroimaging marker that objectively quantifies axonal loss in children with paresis associated with brain injuries. The measurements of hand/leg CST segments using DTI-MAP classifier could discriminate the patterns of motor dysfunction and also selectively detect the corresponding clinical outcome (motor weakness) at the accuracy of 0.78-0.85. The cut-off values of hand/leg CST segments associated with motor weakness might facilitate the objective evaluation of evidence-based treatment and rehabilitation of patients with central paresis. In addition, we also demonstrated an increasing age-related gap in whole brain white matter and CST absolute volumes between the paretic and control groups; and also a novel, biphasic age-related variation of the normalized CST segmental volumes in non-paretic children, which was lacking in the paretic children. This provides new insights into the developmental changes of the human CST during brain maturation, and also into the effects of early brain lesions affecting the motor system.

Previous studies have investigated diffusion metric changes within the CST in hemiplegic children [18-20]. Jung et al. [18] reported that fractional anisotropy (FA) and apparent diffusion coefficient (ADC) are preserved in CST of both affected and unaffected hemisphere in hemiplegic patients having impaired fine motor control but no definite motor weakness. This report suggested the direct role of CST in definite motor weakness. Also, the recovery of FA in CST of pediatric hemiplegic patients was reported by Baek et al. [20] who demonstrated that the FA value of the more affected CST shows a significant decrease compared to the opposite side at initial and follow up evaluation. The FA values of both CSTs showed a significant increase at follow up compared to the initial evaluation, while more changes were observed on the more affected side, compared with the less affected side. This study suggested that DTI tractography might provide a potential imaging marker that can monitor the progress of CST injury as well as its plasticity in pediatric disorders not limited to hemiplegia [21-24].

Previous studies were limited in that they investigated macrostructural changes in white matter integrity of the *entire* CST bundles; these studies did not provide effective measures of actual axonal loss in specific CST regions associated with limb-specific motor dysfunction [25]. In the present study, we utilized the recently developed DTI-MAP classifier to segment specific CST volumes associated with hand and motor functions. Thus, actual decreases in fiber volumes of separate CST segments affected by brain injuries could be utilized to demonstrate their functional correlates with clinical outcomes.

In addition to accurate detection of limb-specific motor fiber abnormalities in children with motor deficit, we have also found a non-linear age-related variation of the CST segmental volumes in the control subjects. This bi-phasic change, likely indicating a normal maturation of CST segments, was only observed after normalization to whole-brain white matter volume, but not in absolute volumes that showed a moderate age-related increase. The use of both absolute and normalized CST volumes provided a more comprehensive insight into normal CST maturation; although normalized volumes are affected by whole-brain changes, they have the advantage of providing data more specific for CST after taking out the effect

of global white matter variations. Therefore, these data refine our recent results demonstrating an age-related decrease of right CST leg segments in children with normal motor functions [16]. The population in the present study had a wider age range (1-20 years vs. 1-14 years in the previous study), and non-linear fitting of normalized volumes demonstrated, for the first time, an early CST-specific age-related increase in both hand and leg motor segments which reached their maxima around age 5-6 years, followed by a sharp decline in the next 5-6 years of age, and subsequently a flattening out after adolescence. Similar to our previous findings [16], the age-related correlations were the strongest in the right leg-related CST segments. However, the curves showed a similar pattern (although with weaker correlations) in the hand segments, and, to the least degree, in the left leg segment as well. The age-related correlation of hand segments were first found in the present study. This different developmental results of hand segments, as compared to our previous findings [16] may be due to the fact that the CST segmental volume variable was normalized differently in the current study where total supratentorial white matter volume was utilized as a scale factor for NSVR value instead of hemispheric white matter volume. Remarkably, the maturational changes in both absolute and normalized CST segments of hand and leg were lost in the paretic children, indicating an altered maturational curve. This could be further addressed by longitudinal DTI studies.

Several limitations of the present study should be noted. First, this study included 11 young children with focal epilepsy as control subjects due to the difficulty in performing MRI scans on young healthy children (under 4 years old) without sedation. Thus, the age range of the healthy and epilepsy controls was different. Although we utilized ages as covariate in all comparisons, there still may be some degree of statistical confounding from unknown CST changes due to the underlying various neurological conditions. Second, the study included children with a wide age range, including young children as low as 1.5 years of age, whose measured white matter and also CST volumes were considerably smaller than those of older subjects (as illustrated Figure 4). In small brains, same-size voxels cover a larger proportion of brain tissue, thus reducing sensitivity of measuring smaller volumes, such as smaller CST volumes. This may have led to the underestimation of CST volumes in some of the youngest patients, where this issue could be resolved by the use of smaller voxels in future studies. In addition, the study was retrospective, as the data have all been collected by the time our new DTI-MAP classification analysis became available; therefore, the present study was not able to collect formal handedness/footedness measures and also detailed, reliable degree of motor weakness for all subjects. Nevertheless, in our recent study in children with unilateral Sturge-Weber syndrome, we demonstrated that severity of hand motor weakness correlated with the lateralization index of the volume of CST hand motor segments [13]. Future, prospective studies should include full clinical assessment and scoring of motor functions in hand and leg to evaluate the ability of the DTI-MAP classifier to assess the severity of motor dysfunction of the limbs.

5. Conclusion

In conclusion, the present study demonstrated that DTI-MAP analysis is useful to 1) detect decreased CST volumes corresponding to hand and leg motor dysfunction (motor weakness and increased muscle tone), 2) establish cut-off values of hand/leg CST segments that might

indicate hand and leg-specific motor weakness in children, and 3) study normal and abnormal developmental variations of hand- and leg-motor related CST segments. This DTI methodology can be used in future studies to explore functional correlates of differential development of CST segments in hemiparetic children. Finally, DTI-MAP analysis can provide a new tool to detect motor dysfunction at early stage and investigate brain plasticity and altered maturational curves of specific pathways in the developing brain.

Acknowledgments

The study was supported by a grant (NS089659 to J.J) from the National Institute of Neurological Disorders and Stroke. The authors would like to thank all participants and their families for their time and interest in this study.

References

1. Barreca S, Wolf SL, Fasoli S, Bohannon R. Treatment interventions for the paretic upper limb of stroke survivors: a critical review. Neurorehabil Neural Repair. 2003; 17(4):220–6. [PubMed: 14677218]
2. Patten C, Lexell J, Brown HE. Weakness and strength training in persons with poststroke hemiplegia: rationale, method, and efficacy. J Rehabil Res Dev. 2004; 41(3A):293–312. [PubMed: 15543447]
3. Stanley, F.; Blair, E.; Alberman, E. Cerebral palsies: Epidemiology and Causal Pathways (Clinics in Developmental Medicine). Cambridge University Press; Jan 18. 2000
4. Krägeloh-Mann I, Horber V. The role of magnetic resonance imaging in elucidating the pathogenesis of cerebral palsy: a systematic review. Dev Med Child Neurol. 2007; 49(2):144–51. [PubMed: 17254004]
5. Conturo TE, Lori NF, Cull TS, Akbudak E, Snyder AZ, Shimony JS, McKinstry RC, Burton H, Raichle ME. Tracking neuronal fiber pathways in the living human brain. Proc Natl Aca Sci. 1999; 96:10422–10427.
6. Basser PJ, Mattiello J, LeBihan D. MR diffusion tensor spectroscopy and imaging. Biophys J. 1994; 66:259–267. [PubMed: 8130344]
7. Basser PJ. Inferring microstructural features and the physiological state of tissues from diffusion-weighted images. NMR Biomed. 1995; 8:333–344. [PubMed: 8739270]
8. Mori S, Crain BJ, Chacko VP, van Zijl PC. Three-dimensional tracking of axonal projections in the brain by magnetic resonance imaging. Ann Neurol. 1999; 45:265–269. [PubMed: 9989633]
9. Mori S, Kaufmann WE, Pearlson GD, Crain BJ, et al. In vivo visualization of human neural pathways by magnetic resonance imaging. Ann Neurol. 2000; 47:412–414. [PubMed: 10716271]
10. Basser PJ, Pajevic S, Pierpaoli C, Duda J, Aldroubi A. In vivo fiber tractography using DT-MRI data. Magn Reson Med. 2000; 44:625–632. [PubMed: 11025519]
11. Dawnay NA, Glees P. Somatotopic analysis of fibre and terminal distribution in the primate corticospinal pathway. Brain Res. 1986; 391:115–123. [PubMed: 3955378]
12. Jeong JW, Asano E, Yeh FC, Chugani DC, Chugani HT. Independent component analysis tractography combined with a ball-stick model to isolate intravoxel crossing fibers of the corticospinal tracts in clinical diffusion MRI. Magn Reson Med. 2013; 70:441–53. [PubMed: 23001816]
13. Jeong JW, Chugani HT, Juhász C. Localization of function-specific segments of the primary motor pathway in children with Sturge-Weber syndrome: A multimodal imaging analysis. J Magn Reson Imaging. 2013; 38(5):1152–61. [PubMed: 23463702]
14. Jeong JW, Asano E, Brown EC, Tiwari VN, Chugani DC, Chugani HT. Automatic detection of primary motor areas using diffusion MRI tractography: comparison with functional MRI and electrical stimulation mapping. Epilepsia. 2013; 54:1381–90. [PubMed: 23772829]
15. Jeong JW, Asano E, Juhasz C, Chugani HT. Quantification of primary motor pathways using diffusion MRI tractography and its application to predict postoperative motor deficits in children with focal epilepsy. Hum Brain Mapp. 2014; 35(7):16–26.

16. Kamson DO, Juhasz C, Shin J, Behen ME, Guy WC, Chugani HT, Jeong JW. Patterns of structural reorganization of the corticospinal tract in children with Sturge-Weber syndrome. Pediatr Neurol. 2014; 50(4):337–42. [PubMed: 24507695]
17. Kamson DO, Juhasz C, Chugani HT, Jeong JW. Novel diffusion tensor imaging technique reveals developmental streamline volume changes in the corticospinal tract associated with leg motor control. Brain Dev. Epub ahead of print. 10.1016/j.braindev.2014.07.001
18. Jung YJ, Jang SH, Yeo SS, Lee E, Kim S, Lee DG, Kim HS, Son SM. Medial lemniscus lesion in pediatric hemiplegic patients without corticospinal tract and posterior thalamic radiation lesion. Eur Neurol. 2012; 67(4):211–6. [PubMed: 22414658]
19. Jang SH, Byun WM, Han BS, Park HJ, Bai D, Ahn YH, Kwon YH, Lee MY. Recovery of a partially damaged corticospinal tract in a patient with intracerebral hemorrhage: a diffusion tensor image study. Restor Neurol Neurosci. 2006; 24(1):25–9. [PubMed: 16518025]
20. Baek SO, Jang SH, Lee E, Kim S, Hah JO, Park YH, Lee JM, Son SM. CST recovery in pediatric hemiplegic patients: Diffusion tensor tractography study. Neurosci Lett. 2013; 557 PtB:79–83. [PubMed: 24176879]
21. Yu C, Shu N, Li J, Qin W, Jiang T, Li K. Plasticity of the corticospinal tract in early blindness revealed by quantitative analysis of fractional anisotropy based on diffusion tensor tractography. Neurioimge. 2007; 36(2):411–7.
22. Jane SH, Kim SH, Cho SH, Choi BY, Choi YW. Demonstration of motor recovery process in a patient with intracerebral hemorrhage. NeuroRehabilitation. 2007; 22(2):141–5. [PubMed: 17656840]
23. Korzeniewski SJ, Birbeck G, DeLano MC, Potchen MJ, Paneth N. A systematic review of neuroimaging for cerebral palsy. J Child Neurol. 2008; 23(2):216–217. [PubMed: 18263759]
24. Murakami A, Morimoto M, Yamada K, Kizu O, Nishimura A, Nishimura T, Sugimotor T. Fiber-tracking techniques can predict the degree of neurologic impairment for periventricular leukomalacia. Pediatrics. 2008; 122(3):500–6. [PubMed: 18762518]
25. Jones DK, Knösche TR, Turner R. White matter integrity, fiber count, and other fallacies: The do's and don'ts of diffusion MRI. Neuroimage. 2013; 73:239–54. [PubMed: 22846632]

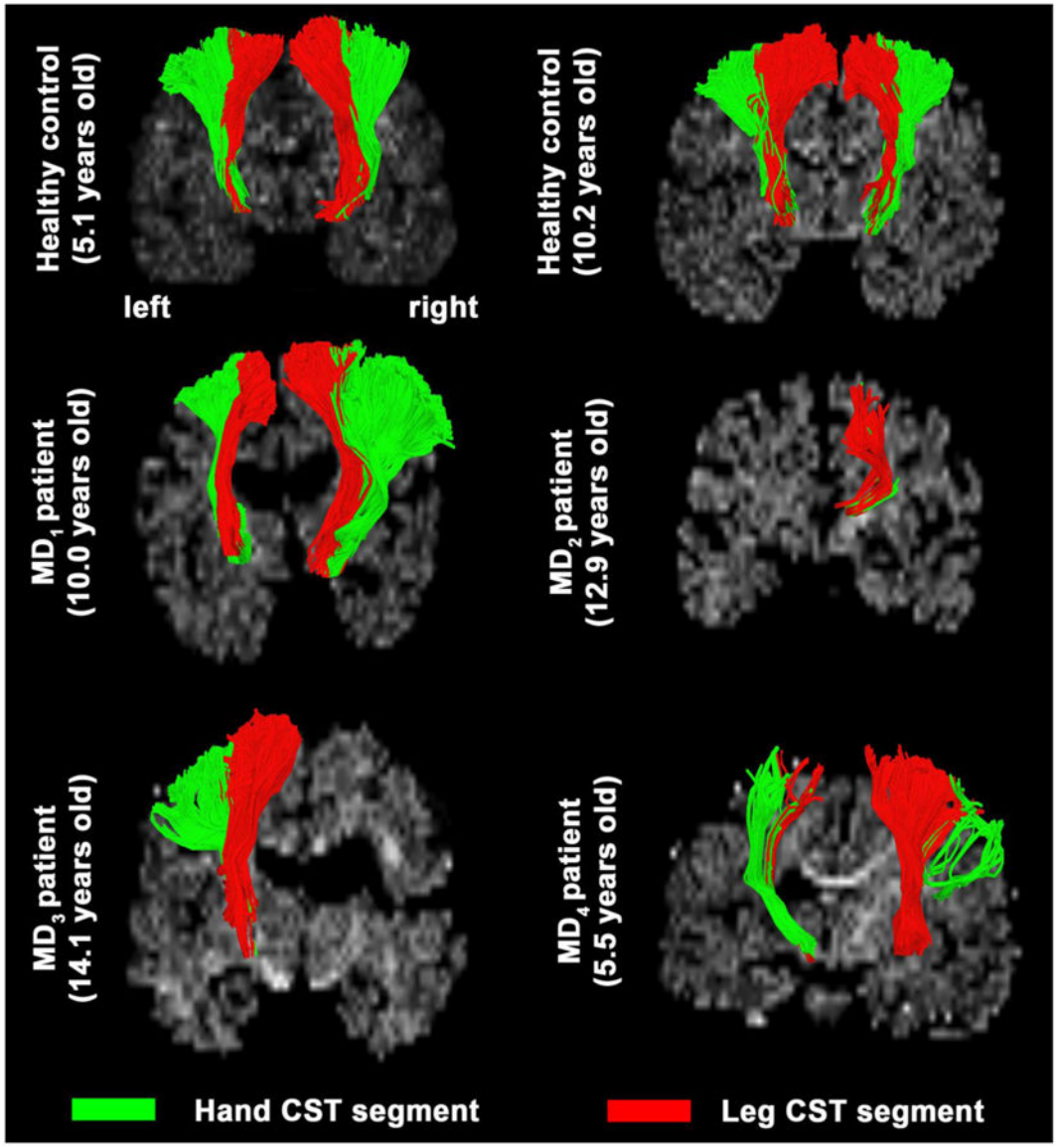

Figure 1.

Representative examples of CST segments, Hand/arm (green) and Leg/trunk (red). The segments were obtained using DTI-MAP classifier from age-gender matched controls (1st row) and four children with central motor dysfunction (2^{nd} and 3^{rd} row: MD_1 of a boy with the most extensive motor weakness in both hands and legs on both sides, MD_2 of a boy with motor weakness in the left hand and leg, MD_3 of a boy with motor weakness in the right hand and leg, MD_4 of a boy with motor weakness in both hands but not legs, respectively).

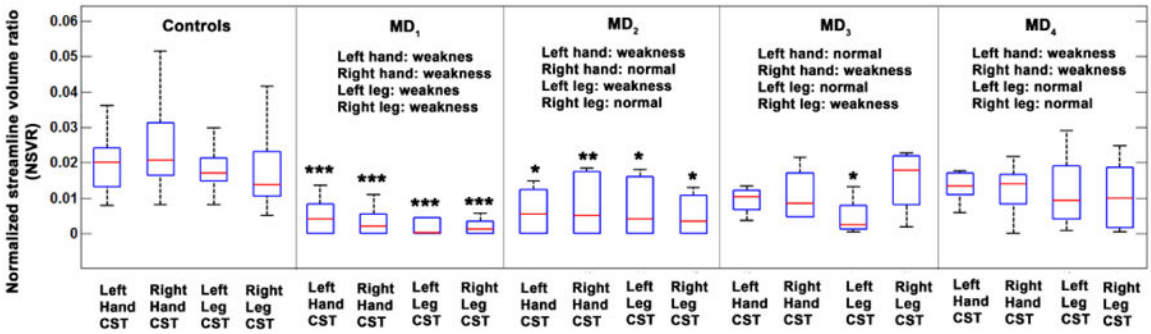

Figure 2.

Box plots showing the significantly decreased NSVR values of four CST segments in 4 subgroups of motor dysfunction patients. Each box has lines at the values of the lower quartile (blue colored), median (red colored), and upper quartile (blue colored). The black colored whiskers are lines extending from each end of the quartiles to show the complete extent of the data. For each ANOVA comparison with healthy controls, *, **, and *** indicate corrected $p < 0.05$, 0.005, and 0.001, respectively.

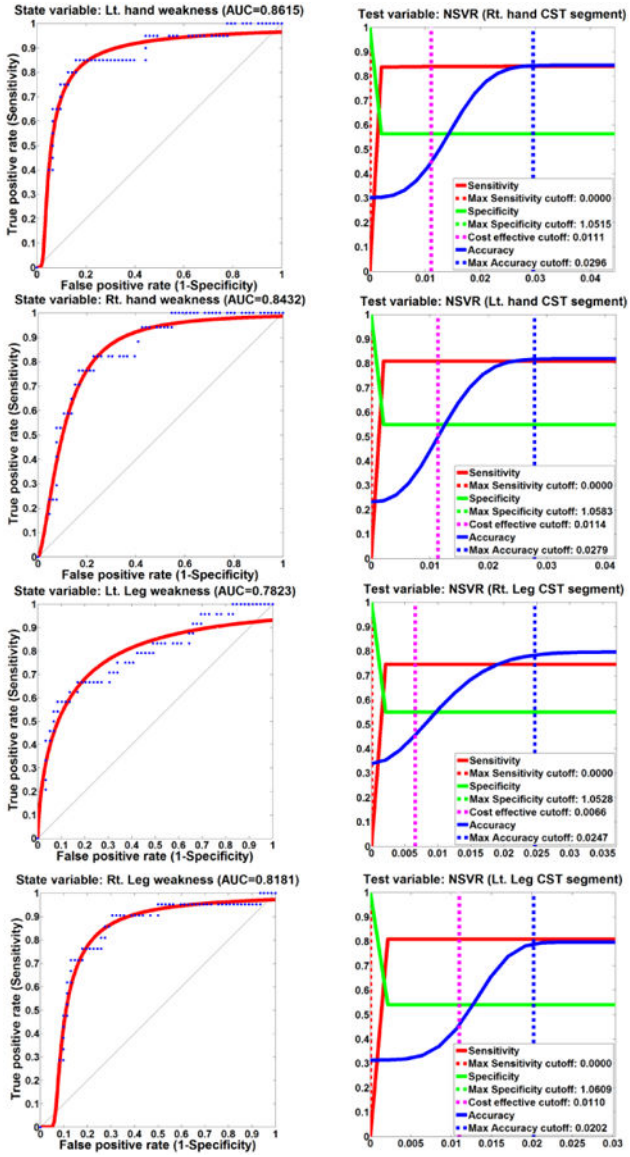

Figure 3.

ROC curves (left column) and cut-off values (right column) of four DTI NSVR values to detect increased motor weakness in MD children.

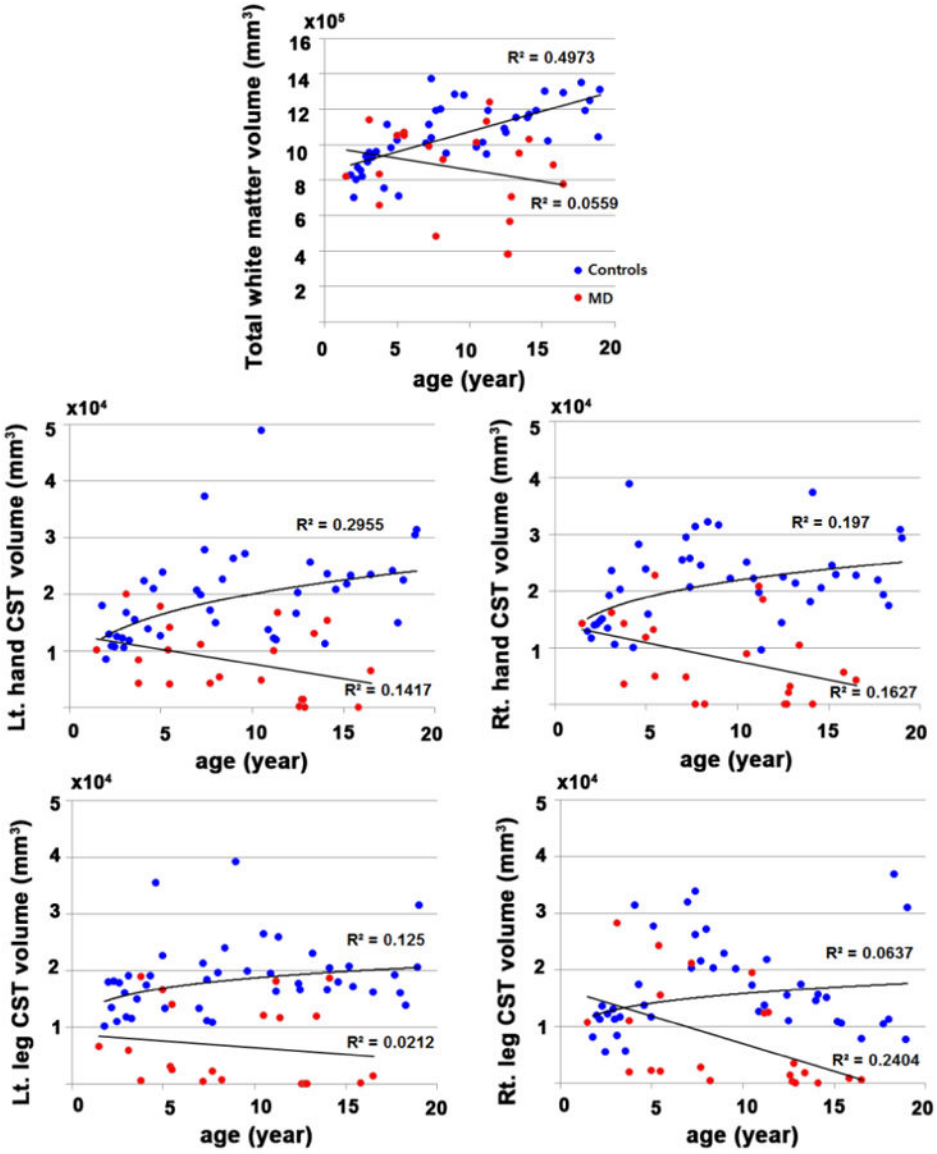

Figure 4.

Scatter plots of total white matter volume and CST segmental volumes by age. Compared with controls, MD children showed no age-related maturation of total white matter and CST segmental volumes. The right leg CST volumes showed a significant age-related decline in the paretic group (p=0.02).

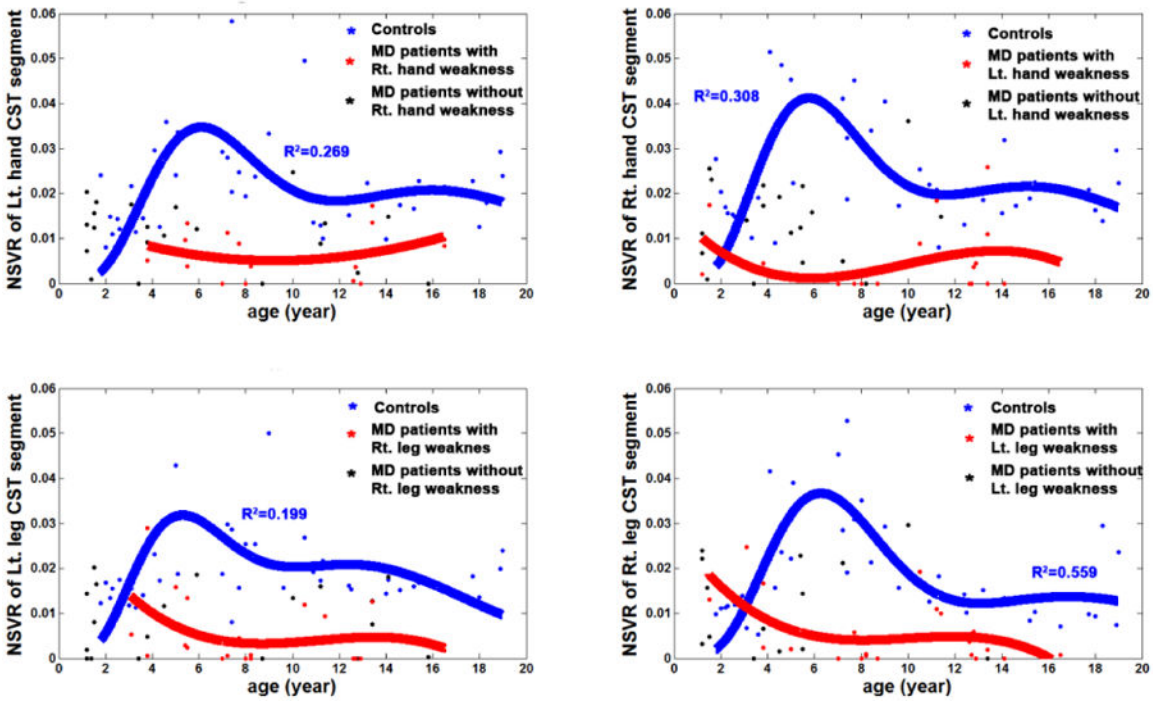

Figure 5.

Age-related changes in NSVR values of controls and MD children. An exponential fitting was applied to estimate the cascaded exponential decline across ages of 42 controls. (i.e., $NSVR(age) = \alpha_1 \cdot age^{-\beta 1} \cdot \exp(-age/\tau_1) - \alpha_2 \cdot age^{-\beta 2} \cdot \exp(-age/\tau_2)$ where $\alpha_{1,2}$, $\beta_{1,2}$, and $\tau_{1,2}$ were estimated with nonlinear least square fit.).

Table 1

Motor dysfunction (MD) subgroups classified by the presence and distribution of motor weakness.

Subgroup	Sample size (n)	Extremity			
		Left Hand	Right Hand	Left Leg	Right Leg
MD_1	10	Yes	Yes	Yes	Yes
MD_2	6	Yes	No	Yes	No
MD_3	4	No	Yes	No	Yes
MD_4	5	Yes	Yes	No	No

Table 2

Statistical significance between healthy controls and 4 MD subgroups obtained from separate ANOVA analyses.

NSVR	Statistics	MD_1	MD_2	MD_3	MD_4
	Cohen's d	2.42	1.54	1.19	1.08
Left hand CST	F-statistic	12.49	5.74	2.93	2.44
	P-value	<0.0001	0.006	0.064	0.082
	Cohen's d	2.76	1.68	1.43	1.18
Right hand CST	F-statistic	16,71	6.56	1.10	2.89
	P-value	<0.0001	0.003	0.090	0.066
	Cohen's d	2.52	1.43	2.09	0.80
Left leg CST	F-statistic	12.66	4.10	4.35	1.51
	P-value	<0.0001	0.023	0.019	0.232
	Cohen's d	1.78	1.18	1.03	0.58
Right leg CST	F-statistic	7.95	4.41	1.34	1.28
	P-value	0.001	0.018	0.075	0.288